

A nonperturbative study of three-dimensional ϕ^4 theory

Mark Windoloski¹
University of Massachusetts
Amherst, MA 01003

The spherical field formalism—a nonperturbative approach to quantum field theory—was recently introduced and applied to ϕ^4 theory in two dimensions. The spherical field method reduces a quantum field theory to a finite-dimensional quantum mechanical system by expanding field configurations in terms of spherical partial wave modes. We extend the formalism to ϕ^4 theory in three dimensions and demonstrate the application of the method by analyzing the phase structure of this theory.

I. INTRODUCTION

Recently a new nonperturbative approach to quantum field theory, called spherical field theory (SFT), has been introduced by Lee [1]. The idea of this approach is to reduce a quantum field theory to a finite-dimensional quantum mechanical system by expanding field configurations using spherical partial wave modes. The dimension of the system is made finite by truncating the partial wave expansion by neglecting high spin waves. The resulting quantum mechanical system can then be analyzed numerically in Euclidean spacetime with the use of diffusion Monte Carlo methods (DMC).

SFT was developed in the context of $(\phi^4)_2$ theory in [1]. The purpose of the present work is to demonstrate that SFT can be extended beyond two-dimensional theories by developing the formalism for $(\phi^4)_3$ theory. In fact, we start out with a general extension of [1] to an integer number of dimensions $N > 2$ and specialize to $N = 3$ when we renormalize the theory.

The paper is organized as follows: We begin by expanding the field configurations in the generating functional for ϕ^4 theory in N dimensions in terms of spherical partial waves and integrating over the angular coordinates in the resulting expression. Then, allowing the radial coordinate to play the role of a time coordinate, we use the Feynman-Kac formula to write the generating functional in terms of a Schrödinger time evolution operator called the spherical-field hamiltonian. Next we apply functional differentiation to the generating

¹email: markw@het2.physics.umass.edu

functional to yield the free two-point correlators of the partial wave fields. Then we discuss the renormalization of $(\phi^4)_3$ in the context of spherical field theory. Finally, to illustrate the application of this new method we model the quantum mechanical system defined by the spherical-field hamiltonian using DMC in order to analyze the phase structure of $(\phi^4)_3$.

Consistent with Magruder’s study of $(\phi^4)_3$ theory [2] we find that the theory undergoes a transition from a broken-symmetry phase to a symmetric phase if the mass-squared parameter μ^2 is negative. In the case of μ^2 positive Magruder’s analysis does not determine if spontaneous symmetry breaking occurs in this theory. Several authors have investigated this question using various nonperturbative methods; the results of their analyses are, however, in disagreement. Cea and Tedesco [3] studied a generalization of the Gaussian effective potential in which they calculated the two-loop corrections to the Gaussian approximation. They found no spontaneous symmetry breaking. In contrast, Stancu [4] used an expansion of the effective potential based on the variational Gaussian effective potential method and found that a phase transition does exist. Peter, Häuser, Thoma and Cassing [5] also found spontaneous symmetry breaking by applying the coupled set of equations of motion for Green functions up to the 4-point level truncated by the use of the cluster expansions for n -point Green functions. With our analysis we find that the theory does not undergo a phase transition if μ^2 is positive—the vacuum remains invariant under the reflection $\phi \rightarrow -\phi$.

For the phase transition observed for $\mu^2 < 0$ we compute the critical coupling and the critical exponents ν and β . Recent calculations of the critical exponents for the three-dimensional Ising universality class—to which $(\phi^4)_3$ is believed to belong—have been performed to a very high level of precision using various approaches such as Monte Carlo simulations of ϕ^4 lattice models (MC) [6], high temperature series expansions (HT) [7], $d = 3$ expansions and ϵ -expansions [8]. At the present early stage in the development of SFT we are limited by the underdeveloped state of the Monte Carlo algorithms available to model the dynamics of systems governed by spherical-field hamiltonians ² and so we do not intend our estimates of ν and β to be competitive with the state-of-the-art results. Rather, we compare our estimates with them in an attempt to build confidence in this new method.

There are important advantages to the spherical field formalism. The method maintains exact rotational invariance and it can be generalized to other geometries as was recently done with a study of quantum field theory on the noncommutative plane [10]. Most importantly, it is a continuum approach rather than a discrete approximation method and so it is free of certain problems which arise in lattice calculations such as fermion doubling [11].

²This state of affairs is not restricted to SFT. For example, see [9] for a relevant discussion in the context of hamiltonian lattice gauge theory.

II. THE GENERATING FUNCTIONAL

The first step in the spherical field theory approach is to perform a spherical partial wave expansion of the fields in the generating functional.³ In N -dimensional Euclidean space the generating functional for ϕ^4 theory is given by

$$Z[\mathcal{J}] = \int \mathcal{D}\phi \exp \left\{ \int d^N \mathbf{x} [\mathcal{L} + \mathcal{J}\phi] \right\} \quad (1)$$

where

$$\mathcal{L} = -\frac{1}{2} \sum_{i=1}^N (\partial_i \phi)^2 - \frac{\mu^2}{2} \phi^2 - \frac{g}{4!} \phi^4. \quad (2)$$

We express the cartesian coordinates in terms of hyperspherical coordinates,

$$\begin{aligned} x_1 &= t \sin \vartheta_1 \sin \vartheta_2 \cdots \sin \vartheta_{N-2} \cos \varphi \\ x_2 &= t \sin \vartheta_1 \sin \vartheta_2 \cdots \sin \vartheta_{N-2} \sin \varphi \\ x_3 &= t \sin \vartheta_1 \sin \vartheta_2 \cdots \cos \vartheta_{N-2} \\ &\vdots \\ x_{N-1} &= t \sin \vartheta_1 \cos \vartheta_2 \\ x_N &= t \cos \vartheta_1, \end{aligned} \quad (3)$$

and decompose the field ϕ and the source \mathcal{J} into partial waves:

$$\phi(\mathbf{x}) = \sum_{\boldsymbol{\lambda}, m} \phi_{\boldsymbol{\lambda}, m}(t) Y_{\boldsymbol{\lambda}, m}(\Omega), \quad (4)$$

$$\mathcal{J}(\mathbf{x}) = \sum_{\boldsymbol{\lambda}, m} \mathcal{J}_{\boldsymbol{\lambda}, m}(t) Y_{\boldsymbol{\lambda}, m}(\Omega). \quad (5)$$

We have written $\boldsymbol{\lambda}$ for the collection of indices $\lambda_1, \lambda_2, \dots, \lambda_{N-2}$ and Ω for the angular variables $\vartheta_1, \vartheta_2, \dots, \vartheta_{N-2}, \varphi$. Here, and throughout this paper, the sum over $\boldsymbol{\lambda}$ runs over all integer values of the λ_i such that

$$\lambda_1 \geq \lambda_2 \geq \lambda_3 \geq \cdots \geq \lambda_{N-2} \geq 0 \quad (6)$$

and the sum over m runs over all integer values satisfying

$$-\lambda_{N-2} \leq m \leq \lambda_{N-2}. \quad (7)$$

³It should be noted that covariant Euclidean quantization, an important component of the spherical field approach, was introduced in [12].

The $Y_{\boldsymbol{\lambda},m}$ are the N -dimensional hyperspherical harmonics⁴ which reduce to the usual spherical harmonics for $N = 3$. For a useful reference on hyperspherical harmonics as well as the hyperspherical Bessel functions we will need below, see [13].

To express the generating functional in terms of the partial waves we make a change of integration variables in the functional integral of Eq. (1) from ϕ to the set $\{\phi_{\boldsymbol{\lambda},m}\}$. The Jacobian of this transformation is

$$\det \left[\frac{\delta\phi(\boldsymbol{x}')}{\delta\phi_{\boldsymbol{\lambda},m}(t)} \right] = \det \left[\delta(t-t')Y_{\boldsymbol{\lambda},m}(\Omega) \right], \quad (8)$$

which is independent of the $\phi_{\boldsymbol{\lambda},m}(t)$. Thus this change of integration variables simply introduces an overall constant which will be irrelevant for our purposes.

Now, having inserted Eqs. (4) and (5) into Eq. (1), we can simplify the expression for $Z[\mathcal{J}]$ by using the orthogonality condition of the hyperspherical harmonics,

$$\int d\Omega Y_{\boldsymbol{\lambda},m}^*(\Omega)Y_{\boldsymbol{\lambda}',m'}(\Omega) = \delta_{\boldsymbol{\lambda},\boldsymbol{\lambda}'}\delta_{m,m'}, \quad (9)$$

to integrate over Ω in the action. Before we can do this we must eliminate the angular derivatives of the $Y_{\boldsymbol{\lambda},m}$ which appear in the kinetic term of \mathcal{L} . This can be accomplished by integrating this kinetic term by parts to yield

$$-\frac{1}{2} \int d^N\boldsymbol{x} \sum_{i=1}^N (\partial_i\phi)^2 = \frac{1}{2} \int d^N\boldsymbol{x} \phi\Delta\phi \quad (10)$$

where Δ denotes the generalized Laplacian operator which can be written in terms of the generalized angular momentum operator Λ^2 as

$$\Delta = \frac{1}{t^{N-1}} \frac{\partial}{\partial t} t^{N-1} \frac{\partial}{\partial t} - \frac{1}{t^2} \Lambda^2. \quad (11)$$

Now the angular derivatives have been removed since the hyperspherical harmonics are eigenfunctions of Λ^2 satisfying the relation

$$\Lambda^2 Y_{\boldsymbol{\lambda},m}(\Omega) = \ell(\ell + N - 2)Y_{\boldsymbol{\lambda},m}(\Omega) \quad (12)$$

where, for ease of notation, we have written ℓ for λ_1 , the first component of $\boldsymbol{\lambda}$.

In performing the integration over Ω of the interaction term we encounter an integral of the product of four hyperspherical harmonics. Let us make the definition

$$\left[\begin{array}{cccc} \lambda_1 & \lambda_2 & \lambda_3 & \lambda_4 \\ m_1 & m_2 & m_3 & m_4 \end{array} \right]_N \equiv \frac{2\pi^{N/2}}{\Gamma(N/2)} \int d\Omega Y_{\boldsymbol{\lambda}_1,m_1}(\Omega)Y_{\boldsymbol{\lambda}_2,m_2}(\Omega)Y_{\boldsymbol{\lambda}_3,m_3}(\Omega)Y_{\boldsymbol{\lambda}_4,m_4}(\Omega) \quad (13)$$

where the prefactor to the integral, which is the area of an N -dimensional unit sphere, is introduced for later convenience. This integral can be calculated by using the expansion

⁴We use the phase convention $Y_{\boldsymbol{\lambda},m}^*(\Omega) = (-1)^m Y_{\boldsymbol{\lambda},-m}(\Omega)$.

$$Y_{\boldsymbol{\lambda}_1, m_1}(\Omega) Y_{\boldsymbol{\lambda}_2, m_2}(\Omega) = \sqrt{\frac{\Gamma(N/2)}{2\pi^{N/2}}} \sum_{\boldsymbol{\lambda}, m} C_N(\boldsymbol{\lambda}_1, m_1; \boldsymbol{\lambda}_2, m_2; \boldsymbol{\lambda}, m) Y_{\boldsymbol{\lambda}, m}(\Omega) \quad (14)$$

where again a prefactor has been introduced for convenience. The coefficients, $C_N(\boldsymbol{\lambda}_1, m_1; \boldsymbol{\lambda}_2, m_2; \boldsymbol{\lambda}, m)$, have been worked out in [14]. They vanish unless $m_1 + m_2 = m$ and so it follows that $\left[\begin{smallmatrix} \boldsymbol{\lambda}_1 & \boldsymbol{\lambda}_2 & \boldsymbol{\lambda}_3 & \boldsymbol{\lambda}_4 \\ m_1 & m_2 & m_3 & m_4 \end{smallmatrix} \right]_N$ vanishes unless $m_1 + m_2 + m_3 + m_4 = 0$. In particular, for $N = 3$ we have

$$\left[\begin{smallmatrix} \ell_1 & \ell_2 & \ell_3 & \ell_4 \\ m_1 & m_2 & m_3 & m_4 \end{smallmatrix} \right]_3 \equiv (-1)^{m_1+m_2+m_3} \delta_{m_4, -m_1-m_2-m_3} \sum_{\ell=|\ell_1-\ell_2|}^{\ell_1+\ell_2} C_3(\ell_1, m_1; \ell_2, m_2; \ell, m_1+m_2) \quad (15)$$

$$\times C_3(\ell, m_1+m_2; \ell_3, m_3; \ell_4, m_1+m_2+m_3)$$

with

$$C_3(\ell_1, m_1; \ell_2, m_2; \ell, m) = \sqrt{\frac{(2\ell_1+1)(2\ell_2+1)}{(2\ell+1)}} \langle \ell_1, \ell_2; m_1, m_2 | \ell_1, \ell_2; \ell, m \rangle$$

$$\times \langle \ell_1, \ell_2; 0, 0 | \ell_1, \ell_2; \ell, 0 \rangle. \quad (16)$$

With these results we are in a position to write down our final expression for the generating functional. We have

$$Z[\mathcal{J}] \propto \int \left(\prod_{\boldsymbol{\lambda}, m} \mathcal{D}\phi_{\boldsymbol{\lambda}, m} \right) \exp \left\{ \int_0^\infty dt \mathcal{L}_{\mathcal{J}}^{\text{Sph}} \right\} \quad (17)$$

where $\mathcal{L}_{\mathcal{J}}^{\text{Sph}}$ is the spherical-field lagrangian,

$$\mathcal{L}_{\mathcal{J}}^{\text{Sph}} = - \sum_{\boldsymbol{\lambda}, m} (-1)^m \left(\frac{t^{N-1}}{2} \frac{d\phi_{\boldsymbol{\lambda}, -m}}{dt} \frac{d\phi_{\boldsymbol{\lambda}, m}}{dt} \right) \quad (18)$$

$$+ \frac{\mu^2 t^2 + \ell(\ell + N - 2)}{2} t^{N-3} \phi_{\boldsymbol{\lambda}, -m} \phi_{\boldsymbol{\lambda}, m} - t^{N-1} \mathcal{J}_{\boldsymbol{\lambda}, -m} \phi_{\boldsymbol{\lambda}, m}$$

$$- ct^{N-1} \sum_{\boldsymbol{\lambda}_1, m_1} \sum_{\boldsymbol{\lambda}_2, m_2} \sum_{\boldsymbol{\lambda}_3, m_3} \sum_{\boldsymbol{\lambda}_4} \left[\begin{smallmatrix} \boldsymbol{\lambda}_1 & \boldsymbol{\lambda}_2 & \boldsymbol{\lambda}_3 & \boldsymbol{\lambda}_4 \\ m_1 & m_2 & m_3 & -m_1-m_2-m_3 \end{smallmatrix} \right]_N$$

$$\times \phi_{\boldsymbol{\lambda}_1, m_1} \phi_{\boldsymbol{\lambda}_2, m_2} \phi_{\boldsymbol{\lambda}_3, m_3} \phi_{\boldsymbol{\lambda}_4, -m_1-m_2-m_3}$$

and the constant c is defined as

$$c \equiv \frac{g}{4!} \frac{\Gamma(N/2)}{2\pi^{N/2}}. \quad (19)$$

III. THE SPHERICAL-FIELD HAMILTONIAN

With the Feynman-Kac formula we can interpret the functional integral Eq. (17) as a time evolution equation where the radial coordinate t now plays the role of a time parameter.

The Feynman-Kac formula, generalized to include the class of time-dependent interactions relevant here, connects the path integral representation of Euclideanized quantum mechanics to the Schrödinger representation,

$$\int_{\substack{\phi(t_I)=x_I \\ \phi(t_F)=x_F}} \mathcal{D}\phi \exp \left\{ - \int_{t_I}^{t_F} dt \left[\frac{a(t)}{2} \left(\frac{\partial \phi}{\partial t} \right)^2 + V(\phi, t) \right] \right\} \propto \langle x_F | T \exp \left\{ - \int_{t_I}^{t_F} dt H(t) \right\} | x_I \rangle \quad (20)$$

where

$$H(t) = -\frac{1}{2a(t)} \frac{d^2}{dq^2} + V(q, t). \quad (21)$$

We may use this formula to write down the Schrödinger representation of Eq. (17),

$$Z[\mathcal{J}] \propto \langle 0 | T \exp \left\{ - \int_0^\infty dt H_{\mathcal{J}}^{\text{Sph}}(t) \right\} | a \rangle \quad (22)$$

where

$$\begin{aligned} H_{\mathcal{J}}^{\text{Sph}}(t) = & \sum_{\boldsymbol{\lambda}, m} (-1)^m \left(-\frac{1}{2t^{N-1}} \frac{\partial}{\partial q_{\boldsymbol{\lambda}, -m}} \frac{\partial}{\partial q_{\boldsymbol{\lambda}, m}} \right. \\ & + \frac{\mu^2 t^2 + \ell(\ell + N - 2)}{2} t^{N-3} q_{\boldsymbol{\lambda}, -m} q_{\boldsymbol{\lambda}, m} - t^{N-1} \mathcal{J}_{\boldsymbol{\lambda}, -m} q_{\boldsymbol{\lambda}, m} \Big) \\ & + ct^{N-1} \sum_{\boldsymbol{\lambda}_1, m_1} \sum_{\boldsymbol{\lambda}_2, m_2} \sum_{\boldsymbol{\lambda}_3, m_3} \sum_{\boldsymbol{\lambda}_4} \left[\begin{matrix} \boldsymbol{\lambda}_1 & \boldsymbol{\lambda}_2 & \boldsymbol{\lambda}_3 & \boldsymbol{\lambda}_4 \\ m_1 & m_2 & m_3 & -m_1 - m_2 - m_3 \end{matrix} \right]_N \\ & \times q_{\boldsymbol{\lambda}_1, m_1} q_{\boldsymbol{\lambda}_2, m_2} q_{\boldsymbol{\lambda}_3, m_3} q_{\boldsymbol{\lambda}_4, -m_1 - m_2 - m_3} \end{aligned} \quad (23)$$

is a Schrödinger time evolution generator which we will refer to as the spherical-field hamiltonian. Following [1] we take the quantum state at $t_I = 0$ to be a superposition of all possible states with each state equally weighted,

$$|a\rangle \equiv \int_{-\infty}^{\infty} \left(\prod_{\boldsymbol{\lambda}, m} dx_{\boldsymbol{\lambda}, m} \right) |\{x_{\boldsymbol{\lambda}', m'}\}\rangle. \quad (24)$$

In the set $\{x_{\boldsymbol{\lambda}', m'}\}$, the λ'_i and m' take all integer values satisfying the inequalities (6) and (7) respectively. Note that, with this notation,

$$q_{\boldsymbol{\lambda}, m} |\{x_{\boldsymbol{\lambda}', m'}\}\rangle = x_{\boldsymbol{\lambda}, m} |\{x_{\boldsymbol{\lambda}', m'}\}\rangle. \quad (25)$$

The proper quantum state for $t_F \rightarrow \infty$ is the ground state, $|0\rangle$.

We are faced with the difficulty that the spherical-field hamiltonian is written as an infinite series. In practice we cut this series off by neglecting partial waves with spin higher than some value we call J_{\max} . Such an approximation is justified because, as pointed out in [1], the high spin partial waves correspond to high tangential momentum modes so that a partial-wave cutoff J_{\max} corresponds to a momentum cutoff

$$\Lambda^2 \sim \frac{J_{\max}^2}{t^2}. \quad (26)$$

Therefore the high spin modes will decouple from the theory, just as other high momentum effects, if the theory is renormalized to remove ultraviolet divergences. Below, we will describe the proper method of renormalizing $(\phi^4)_3$ in the context of spherical field theory, but to do so we need to derive an expression for the free two-point correlators of the partial wave fields which can then be used to evaluate the spherical-field version of Feynman diagrams.

IV. CORRELATORS

Correlation functions for partial waves can be computed from the generating functional. We begin by writing the generating functional Eq. (1) as a power series,

$$\frac{Z[\mathcal{J}]}{Z[0]} = 1 + \frac{1}{2} \int \frac{d^N \mathbf{p} d^N \mathbf{x} d^N \mathbf{y}}{(2\pi)^N} e^{-i\mathbf{p} \cdot (\mathbf{x} - \mathbf{y})} \mathcal{J}(\mathbf{x}) \mathcal{J}(\mathbf{y}) f(\mathbf{p}^2) + \dots \quad (27)$$

where $f(\mathbf{p}^2)$ is the ϕ propagator,

$$f(\mathbf{p}^2) = \int d^N \mathbf{x} e^{i\mathbf{p} \cdot \mathbf{x}} \langle 0 | \phi(\mathbf{x}) \phi(0) | 0 \rangle. \quad (28)$$

We insert the partial wave expansion of $\mathcal{J}(\mathbf{x})$ given in Eq. (5) and expand the plane waves with

$$e^{-i\mathbf{p} \cdot \mathbf{x}} = (N-2)!! \frac{2\pi^{N/2}}{\Gamma(N/2)} \sum_{\boldsymbol{\lambda}, m} (-i)^\ell j_{N,\ell}(kt) Y_{\boldsymbol{\lambda}, m}^*(\Omega_k) Y_{n,m}(\Omega_t) \quad (29)$$

where $k \equiv |\mathbf{p}|$, $t \equiv |\mathbf{x}|$ and $j_{N,n}$ is the hyperspherical Bessel function of order n ,

$$j_{N,n}(x) = \frac{\Gamma(\alpha) 2^{\alpha-1} J_{n+\alpha}(x)}{(N-4)!! t^\alpha}, \quad (30)$$

where $\alpha \equiv \frac{N-2}{2}$. Then we can perform the angular integration in Eq. (27) to obtain

$$\begin{aligned} \frac{Z[\mathcal{J}]}{Z[0]} = 1 + \frac{1}{2^{N-1}} \left[\frac{(N-2)!!}{\Gamma(N/2)} \right]^2 \sum_{\boldsymbol{\lambda}, m} \int_0^\infty dk dt_x dt_y \quad (31) \\ \times k^{N-1} t_x^{N-1} t_y^{N-1} f(k^2) \mathcal{J}_{\boldsymbol{\lambda}, -m}(t_x) \mathcal{J}_{\boldsymbol{\lambda}, m}(t_y) j_{N,\ell}(kt_x) j_{N,\ell}(kt_y) + \dots \end{aligned}$$

From this expression we may calculate the two-point correlator for $\phi_{\boldsymbol{\lambda}, m}$,

$$\begin{aligned}
\langle 0 | \phi_{\boldsymbol{\lambda},-m}(t_1) \phi_{\boldsymbol{\lambda},m}(t_2) | 0 \rangle &= \frac{1}{Z[0]} \left(\frac{\delta}{t_1^{N-1} \delta \mathcal{J}_{\boldsymbol{\lambda},m}(t_1)} \frac{\delta}{t_2^{N-1} \delta \mathcal{J}_{\boldsymbol{\lambda},-m}(t_2)} Z[\mathcal{J}] \right) \Bigg|_{\mathcal{J}=0} \\
&= \frac{1}{2^{N-2}} \left[\frac{(N-2)!!}{\Gamma(N/2)} \right]^2 (-1)^m \int_0^\infty dk k^{N-1} f(k^2) j_{N,\ell}(kt_1) j_{N,\ell}(kt_2).
\end{aligned} \tag{32}$$

The free-field two-point $\phi_{\boldsymbol{\lambda},m}$ correlator is obtained by inserting the free propagator $f(k^2) = \frac{1}{k^2 + \mu^2}$ into Eq. (32). The result is

$$\begin{aligned}
\langle 0 | \phi_{\boldsymbol{\lambda},-m}(t_1) \phi_{\boldsymbol{\lambda},m}(t_2) | 0 \rangle &= (-1)^m \mu^{2\alpha} \left[\frac{(N-2)!! \Gamma(\alpha)}{2\Gamma(N/2)} \right]^2 \\
&\quad \times [\theta(t_1 - t_2) k_{N,\ell}(\mu t_1) i_{N,\ell}(\mu t_2) + \theta(t_2 - t_1) k_{N,\ell}(\mu t_2) i_{N,\ell}(\mu t_1)],
\end{aligned} \tag{33}$$

where $k_{N,n}$ and $j_{N,n}$ are the hyperspherical modified Bessel functions of order n which are given by

$$k_{N,n}(x) = \frac{K_{n+\alpha}(x)}{\Gamma(\alpha) 2^{\alpha-1} (N-4)!! t^\alpha}, \tag{34}$$

$$i_{N,n}(x) = \frac{\Gamma(\alpha) 2^{\alpha-1} I_{n+\alpha}(x)}{(N-4)!! t^\alpha}. \tag{35}$$

V. RENORMALIZATION

Hereafter we will specialize to three dimensions.⁵ In this case the theory can be made finite by adding a mass counterterm to the lagrangian Eq. (2) which subtracts all primitively divergent self-energy diagrams. In three dimensions there are two such diagrams. One of these, shown in Fig. 1(a), is local and so it is straightforward to write down the appropriate counterterms corresponding to this diagram in the context of spherical field theory. We must explicitly subtract the contribution of all diagrams having the form shown in Fig. 2(a). Using Eq. (33), and recalling the spherical-field lagrangian Eq. (18), we find that the counterterm which corresponds to a diagram of this form is proportional to

$$(-1)^{m'} \mu c t^2 \left[\begin{matrix} \ell & \ell & \ell' & \ell' \\ m & -m & m' & -m' \end{matrix} \right] k_{\ell'}(\mu t) i_{\ell'}(\mu t) \phi_{\ell,-m}(t) \phi_{\ell,m}(t). \tag{36}$$

The proportionality constant is a product of two factors. One is the degeneracy of the quartic term in the lagrangian which gives rise to such a diagram, or equivalently the number of distinct permutations of the columns in the bracket symbol. The other is the number of possible contractions of this quartic term which correspond to the diagram.

The other divergent diagram is the so-called sunset diagram shown in Fig. 1(b). This divergence can also be eliminated by using a local mass counterterm. In ordinary field theory

⁵We will no longer write dimension subscripts, *i.e.* $k_{3,n}(x)$ will be written as $k_n(x)$, etc.

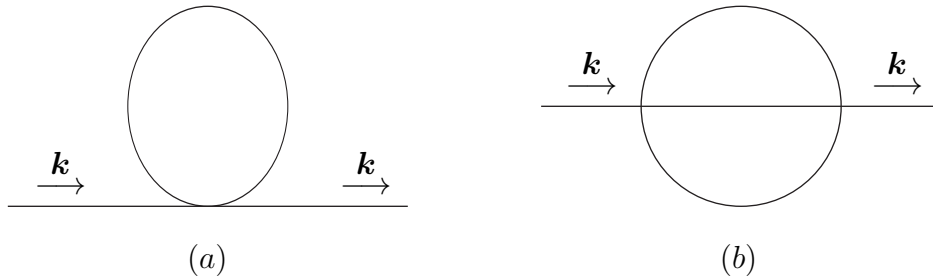


FIG. 1. The primitively divergent self-energy diagrams in ordinary perturbation theory.

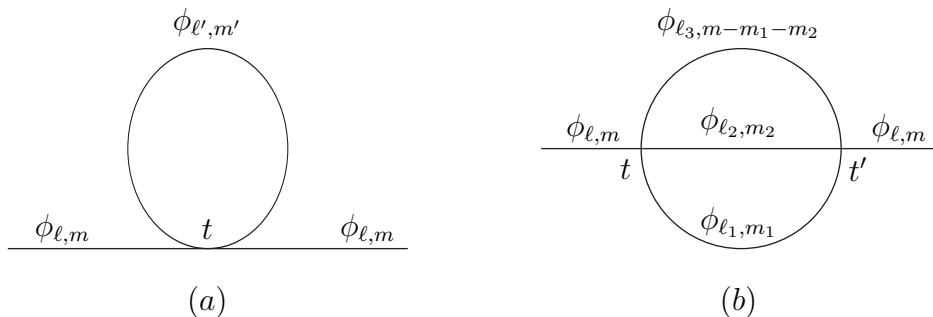


FIG. 2. The primitively divergent self-energy diagrams in spherical field theory.

one finds that the divergence is logarithmic, and so a single subtraction at any value of k^2 will cancel it. It is natural to choose $k^2 = 0$. In the context of spherical field theory, we work in position space. To obtain a local counterterm we must consider all diagrams of the form shown in Fig. 2(b) and we must integrate over the coordinate of one of the vertices, say t' . However, we must do this in such a way as to keep our renormalization condition translationally and rotationally invariant.

Working again in ordinary perturbation theory, we consider the sum of the sunset diagram and its counterterm in position space,

$$\Sigma(\mathbf{x}, \mathbf{x}') = \sigma(\mathbf{x}, \mathbf{x}') - \delta\sigma(\mathbf{x}) \delta(\mathbf{x} - \mathbf{x}'). \quad (37)$$

Here, the first term on the right hand side denotes the diagram itself and the second term denotes the counterterm. For convenience, we rewrite the second term as $\delta\sigma(\mathbf{x}, \Omega_{\mathbf{x}'} \frac{\delta(t-t')}{t^2})$ absorbing the angular part of the delta function into $\delta\sigma$. We want the amplitude to vanish at $k^2 = 0$. To impose this condition in a translationally and rotationally invariant way we demand that

$$\int d^3\mathbf{x}' \Sigma(\mathbf{x}, \mathbf{x}') e^{-i\mathbf{k}\cdot(\mathbf{x}-\mathbf{x}')} = f(k^2) \quad (38)$$

where $f(k^2)$ is some function of k^2 which vanishes as $k^2 \rightarrow 0$.

We can move the exponential factor independent of \mathbf{x}' to the right hand side of the equation and make use of Eq. (29) to obtain the condition

$$\int d^3\mathbf{x}' j_\ell(kt') Y_{\ell,m}(\Omega_{\mathbf{x}'}) \Sigma(\mathbf{x}, \mathbf{x}') = j_\ell(kt) Y_{\ell,m}(\Omega_{\mathbf{x}}) f(k^2) \quad (39)$$

which must hold for all possible values of ℓ and m . Finally, we take the limit $k^2 \rightarrow 0$. In this limit, $j_\ell(kt) \propto (kt)^\ell$ and so we have

$$\int d\Omega_{\mathbf{x}'} Y_{\ell,m}(\Omega_{\mathbf{x}'}) \delta\sigma(\mathbf{x}, \Omega_{\mathbf{x}'}) = \frac{1}{t^\ell} \int_0^\infty dt' t'^{(\ell+2)} \int d\Omega_{\mathbf{x}'} Y_{\ell,m}(\Omega_{\mathbf{x}'}) \sigma(\mathbf{x}, \mathbf{x}') \quad (40)$$

for all ℓ and m . This relation tells us the proper way to integrate a diagram of the form of Fig. 2(b) over t' in order to obtain the corresponding counterterm. With this information and again using Eq. (33), we can write down this counterterm. It is proportional to

$$-\frac{1}{2} (-1)^m c^2 t^2 \left[\begin{matrix} \ell_1 & \ell_2 & \ell_3 & \ell \\ m_1 & m_2 & m-m_1-m_2 & -m \end{matrix} \right]^2 I_{\ell_1, \ell_2, \ell_3}^{(\ell)}(\mu t) \phi_{\ell, -m}(t) \phi_{\ell, m}(t) \quad (41)$$

where

$$I_{\ell_1, \ell_2, \ell_3}^{(\ell)}(x) = k_{\ell_1}(x) k_{\ell_2}(x) k_{\ell_3}(x) \frac{1}{x^\ell} \int_0^x dx' x'^{(\ell+2)} i_{\ell_1}(x') i_{\ell_2}(x') i_{\ell_3}(x') \quad (42)$$

$$+ i_{\ell_1}(x) i_{\ell_2}(x) i_{\ell_3}(x) \frac{1}{x^\ell} \int_x^\infty dx' x'^{(\ell+2)} k_{\ell_1}(x') k_{\ell_2}(x') k_{\ell_3}(x').$$

Again, the proportionality constant is a product of two factors. Each diagram of the form of Fig. 2(b) arises from the product of a quartic term from the lagrangian Eq. (18) evaluated at coordinate t and the same quartic term evaluated at coordinate t' . Therefore, one factor in the proportionality constant is the square of the degeneracy of this quartic term. The other factor is the number of possible contractions of the product of these quartic terms which correspond to the diagram.

VI. THE PHASE TRANSITION

In [2], Magruder proved the existence of a phase transition in $(\phi^4)_3$ theory by extending Chang's proof [15] for $(\phi^4)_2$ theory. Let us briefly recall Magruder's analysis. Consider the two lagrangians:

$$\mathcal{L}_+ = \frac{1}{2} (\partial_\mu \phi)(\partial^\mu \phi) - \frac{1}{2} \mu_+^2 \phi^2 - 4\pi c \phi^4 + \frac{1}{2} \delta \mu_+^2 \phi^2, \quad (43)$$

$$\mathcal{L}_- = \frac{1}{2} (\partial_\mu \phi)(\partial^\mu \phi) + \frac{1}{4} \mu_-^2 \phi^2 - 4\pi c \phi^4 + \frac{1}{2} \delta \mu_-^2 \phi^2$$

where μ_+^2 and μ_-^2 are both positive parameters. The mass counterterms, $\delta \mu_+^2$ and $\delta \mu_-^2$, are chosen so that the theories are properly renormalized using the same conditions we have used above. Expressed in terms of a momentum cutoff Λ they are defined as

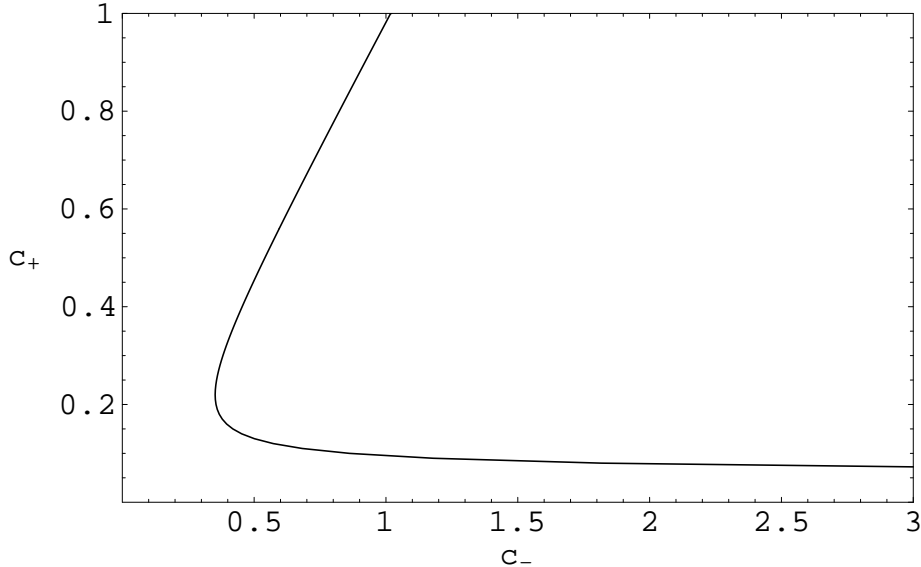


FIG. 3. The functional relation between $c_+ \equiv \frac{c}{\mu_+}$ and $c_- \equiv \frac{c}{\mu_-}$ as given by Eq. (45).

$$\begin{aligned}\delta\mu_+^2 &= 12c(\Lambda - \mu_+) + 96c^2 \ln\left(\frac{\mu_+}{\Lambda}\right), \\ \delta\mu_-^2 &= 12c(\Lambda - \mu_-) + 96c^2 \ln\left(\frac{\mu_-}{\Lambda}\right).\end{aligned}\tag{44}$$

The two lagrangians differ in the sign of their mass terms so that in the weak coupling limit the theory defined by \mathcal{L}_+ has a vacuum with manifest symmetry under the reflection $\phi \rightarrow -\phi$ while the theory defined by \mathcal{L}_- has a vacuum with broken symmetry.

The two lagrangians are identical if the parameters of the theories are chosen such that

$$-\mu_+^2 + \delta\mu_+^2 = \frac{1}{2}\mu_-^2 + \delta\mu_-^2.\tag{45}$$

The solution to this equation, shown graphically in Fig. 3, gives $c_+ \equiv \frac{c}{\mu_+}$ as a function of $c_- \equiv \frac{c}{\mu_-}$. This solution has the property that where \mathcal{L}_+ and \mathcal{L}_- overlap they are inversely related: a strong-coupling theory defined by \mathcal{L}_- is dual to a weak-coupling theory defined by \mathcal{L}_+ . This implies that the theory defined by \mathcal{L}_- undergoes a phase transition from a vacuum with broken symmetry to one with manifest symmetry at some finite value of the coupling strength, $c_- = c_-^{\text{crit}}$. However, Fig. 3 shows that there is no overlap between the two theories for $c_- \lesssim 0.3522$. Therefore, if c_-^{crit} is below this value the theory defined by \mathcal{L}_+ will have a vacuum with manifest symmetry for *any* value of c_+ . On the other hand, if $c_-^{\text{crit}} \gtrsim 0.3522$ then there is a finite range of intermediate coupling strengths for which the theory defined by \mathcal{L}_+ will have a vacuum with broken symmetry. Since this approach cannot tell us the value of c_-^{crit} , it cannot determine whether or not spontaneous symmetry breaking exists in the theory defined by \mathcal{L}_+ .

We can bring the method of spherical field theory to bear on this question by studying the quantum mechanical system defined by the spherical-field hamiltonian. The appropriate hamiltonian is found by adding the two counterterms discussed above to the spherical-field

hamiltonian given by Eq. (23) and setting $\mathcal{J} = 0$. We can do this for the Euclideanized theory corresponding to \mathcal{L}_- as easily as for the one corresponding to \mathcal{L}_+ since the renormalization procedure is the same for both theories as indicated by Eq. (44). The same counterterms, Eqs. (36) and (41), apply in both cases. To avoid the complication of working with a time-dependent hamiltonian we have chosen to investigate the original three-dimensional system on a spherical surface of radius R . Then we may set $t = R$ in the spherical-field hamiltonian, rendering it time-independent. The full field theory result is recovered in the limit $J_{\max} \rightarrow \infty$, $R \rightarrow \infty$.

As an example, we display the spherical-field hamiltonian corresponding to \mathcal{L}_+ for $J_{\max} = 1$:

$$\begin{aligned}
H = & -\frac{1}{2R^2} \left(\frac{\partial^2}{\partial q_{0,0}^2} + \frac{\partial^2}{\partial q_{1,0}^2} + \frac{\partial^2}{\partial q_{1,s1}^2} + \frac{\partial^2}{\partial q_{1,a1}^2} \right) + \frac{\mu^2 R^2}{2} q_{0,0}^2 + \frac{\mu^2 R^2 + 2}{2} (q_{1,0}^2 + q_{1,s1}^2 + q_{1,a1}^2) \\
& + cR^2 \left[q_{0,0}^4 + 6q_{0,0}^2 (q_{1,0}^2 + q_{1,s1}^2 + q_{1,a1}^2) + \frac{9}{5} (q_{1,0}^2 + q_{1,s1}^2 + q_{1,a1}^2)^2 \right] \\
& - 6\mu cR^2 [k_0(\mu R)i_0(\mu R) + 3k_1(\mu R)i_1(\mu R)] (q_{1,0}^2 + q_{1,s1}^2 + q_{1,a1}^2) \\
& + 48c^2 R^2 \left[(I_{0,0,0}^{(0)}(\mu R) + 9I_{0,1,1}^{(0)}(\mu R)) q_{0,0}^2 \right. \\
& \left. + 3 \left(I_{0,0,1}^{(1)}(\mu R) + \frac{9}{5} I_{1,1,1}^{(1)}(\mu R) \right) (q_{1,0}^2 + q_{1,s1}^2 + q_{1,a1}^2) \right]
\end{aligned} \tag{46}$$

where

$$q_{1,s1} = \frac{q_{1,1} + q_{1,-1}}{i\sqrt{2}} \quad \text{and} \quad q_{1,a1} = \frac{q_{1,1} - q_{1,-1}}{\sqrt{2}}. \tag{47}$$

The spherical-field hamiltonian corresponding to \mathcal{L}_- for $J_{\max} = 1$ can be obtained from the above expression by letting $\mu^2 \rightarrow -\frac{1}{2}\mu^2$ in the mass terms while leaving the counterterms unchanged. Due to their lengths we will not include the corresponding expressions for higher values of J_{\max} but they can be written down in a straightforward way using Eqs. (23), (36) and (41).

Equipped with the spherical-field hamiltonian we can use the method introduced in [16] to find the vacuum expectation value and the physical mass as a function of the coupling, c . Near the phase transition the behavior of these quantities define the critical exponents β and ν respectively.

We calculate the physical mass in the symmetric phase of the theory by using DMC⁶ to compute the matrix element

$$f(t) = \langle b | q_{0,0} e^{-tH} q_{0,0} | b \rangle, \tag{48}$$

where $|b\rangle$ is any state that is even under the reflection transformation $\phi \rightarrow -\phi$. To see that one can extract the physical mass from $f(t)$ insert a complete set of energy eigenstates $|i\rangle$ corresponding to energy eigenvalues E_i :

⁶A self-contained introductory presentation of DMC is given in [17].

$$f(t) = \sum_i e^{-tE_i} |\langle i | q_{0,0} | b \rangle|^2. \quad (49)$$

Now the contribution of the ground state vanishes in this sum because both $|0\rangle$ and $|b\rangle$ are even under reflection symmetry while $q_{0,0}$ is odd. Therefore, the sum is dominated by the one-particle-at-rest state in the limit $t \rightarrow \infty$. If we shift the energy scale such that $E_0 = 0$ then for large t

$$f(t) \sim e^{-mt}, \quad (50)$$

where m is the physical mass.

Next let us consider the vacuum expectation value. In the broken-symmetry phase of the theory there are two degenerate ground states if the size of the system becomes infinite, *i.e.* $R \rightarrow \infty$. Let us take these two ground states to be $|0^+\rangle$, which is non-zero only for $q_{0,0} > 0$, and $|0^-\rangle$, which is non-zero only for $q_{0,0} < 0$. We choose these such that they are normalized to unity and so that under reflection symmetry they transform from one to the other. Now our task is to calculate the vacuum expectation value $\langle 0^+ | \phi | 0^+ \rangle$. Using translational and rotational invariance we can write this as

$$\langle 0^+ | \phi | 0^+ \rangle = \frac{1}{4\pi} \int d\Omega \langle 0^+ | \phi(t, \theta, \varphi) | 0^+ \rangle = \langle 0^+ | \frac{q_{0,0}}{\sqrt{4\pi}} | 0^+ \rangle. \quad (51)$$

Let us rewrite the operator $q_{0,0}$ in terms of a projection operator,

$$q_{0,0} = \int_{-\infty}^{\infty} dx_{0,0} x_{0,0} |x_{0,0}\rangle \langle x_{0,0}|. \quad (52)$$

Now we have

$$\langle 0^+ | \phi | 0^+ \rangle = \int_0^{\infty} dx_{0,0} x_{0,0} \frac{|\langle x_{0,0} | 0^+ \rangle|^2}{\sqrt{4\pi}} \quad (53)$$

where the lower limit of integration can be taken to be $x_{0,0} = 0$ since $|0^+\rangle$ vanishes for $x_{0,0} < 0$.

The task which remains is to calculate the matrix element which appears in this last expression. To do this we need to know the ground state $|0^+\rangle$. The time evolution operator $\exp(-Ht)$ operating on any state $|b\rangle$ will project out the state of lowest energy as $t \rightarrow \infty$ provided $|b\rangle$ has a non-zero overlap with this lowest-energy state. Since we are working with a system of finite size the vacuum will not be exactly degenerate. For finite R the state that is lowest in energy is the symmetric superposition of $|0^+\rangle$ and $|0^-\rangle$,

$$|0^s\rangle = \frac{1}{\sqrt{2}} (|0^+\rangle + |0^-\rangle). \quad (54)$$

Therefore we have

$$|\langle x_{0,0} | 0^s \rangle|^2 = \lim_{t \rightarrow \infty} \frac{\langle b | e^{-tH} | x_{0,0} \rangle \langle x_{0,0} | e^{-tH} | b \rangle}{\langle b | e^{-2tH} | b \rangle}, \quad (55)$$

where $|b\rangle$ is chosen such that $\langle 0^s | b \rangle$ is not zero. Now, since $|0^+\rangle = \sqrt{2}|0^s\rangle$ for $x_{0,0} > 0$, the vacuum expectation value can be written as

$$\langle 0^+ | \phi | 0^+ \rangle = 2 \int_0^\infty dx_{0,0} x_{0,0} g(x_{0,0}), \quad (56)$$

where

$$g(x_{0,0}) = \frac{|\langle x_{0,0} | 0^s \rangle|^2}{\sqrt{4\pi}}. \quad (57)$$

We can calculate $g(x_{0,0})$ by using DMC to evaluate the right-hand-side of Eq. (55). However, we will not calculate $\langle 0^+ | \phi | 0^+ \rangle$ by integrating $2x_{0,0}g(x_{0,0})$. Instead we will take

$$\langle 0^+ | \phi | 0^+ \rangle = x_{0,0}^{\max} \quad (58)$$

where $x_{0,0}^{\max}$ is the non-negative value of $x_{0,0}$ for which $g(x_{0,0})$ has its maximum value. This approach is justified because $g(x_{0,0})$ becomes sharply peaked as the size of the system becomes large and $g(x_{0,0})$ satisfies

$$\int_{-\infty}^\infty dx_{0,0} g(x_{0,0}) = 2 \int_0^\infty dx_{0,0} g(x_{0,0}) = 1. \quad (59)$$

This approach converges to the same result as integrating $2x_{0,0}g(x_{0,0})$ in the limit $R \rightarrow \infty$, however, as indicated in [16] it is less susceptible to systematic errors for finite values of R .

VII. RESULTS

The results of our DMC calculations are presented in Figs. 4-10. The error bars indicate our best estimate of the error due to statistical fluctuations as well as the contamination of higher energy states in the physical mass calculations.

For the theory defined by \mathcal{L}_+ we have calculated the vacuum expectation value and the physical mass over a range of coupling strengths⁷ from weak coupling ($c \sim 0$) to very strong coupling ($c \sim 1$). This calculation was done with $J_{\max} = 10$ and $R = 3$ which corresponds to $(J_{\max} + 1)^2 = 121$ partial wave modes and a spherical surface of area $4\pi R^2 = 36\pi$. The vacuum expectation value is found to remain zero, *i.e.* the function $g(x_{0,0})$ has a single maximum at $x_{0,0} = 0$, throughout this range. Furthermore, as shown in Fig. 4, the physical mass begins near unity at weak coupling and consistently grows larger as the coupling strength is increased to large values. We would expect the physical mass to vanish at the point where $\phi \rightarrow -\phi$ reflection symmetry is spontaneously broken. Our results clearly show that there is no phase transition in the theory corresponding to \mathcal{L}_+ .

On the other hand, our results do confirm the phase transition expected for the theory defined by \mathcal{L}_- . We calculated the vacuum expectation value and the physical mass using

⁷We work in units such that $\mu = 1$.

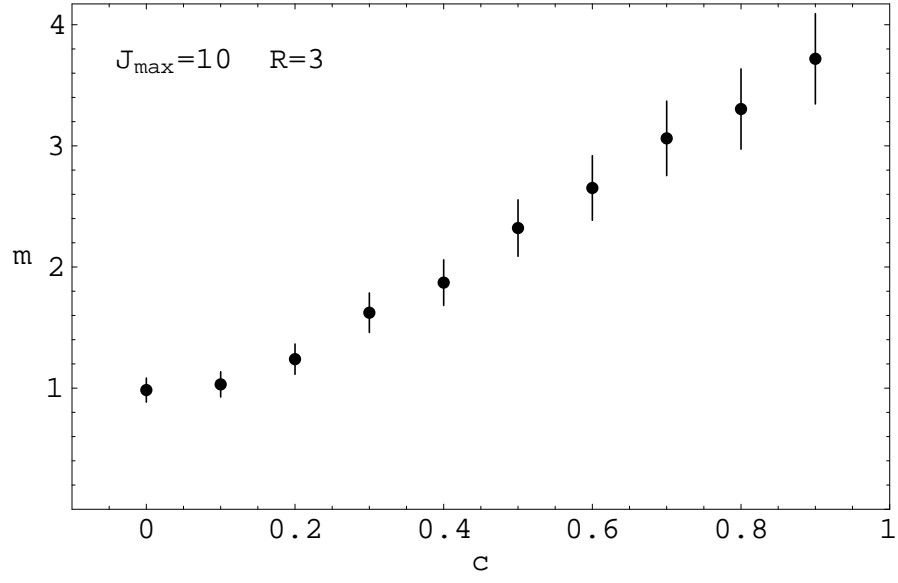


FIG. 4. m as a function of c for the theory defined by \mathcal{L}_+ with $J_{\max} = 10$, $R = 3$.

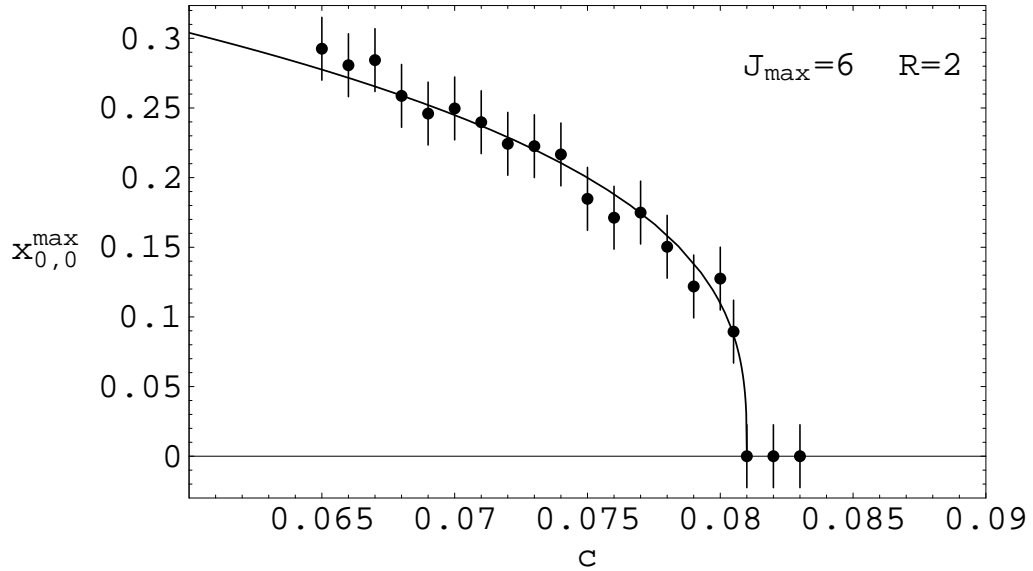


FIG. 5. $x_{0,0}^{\max}$ as a function of c for the theory defined by \mathcal{L}_- with $J_{\max} = 6$, $R = 2$.

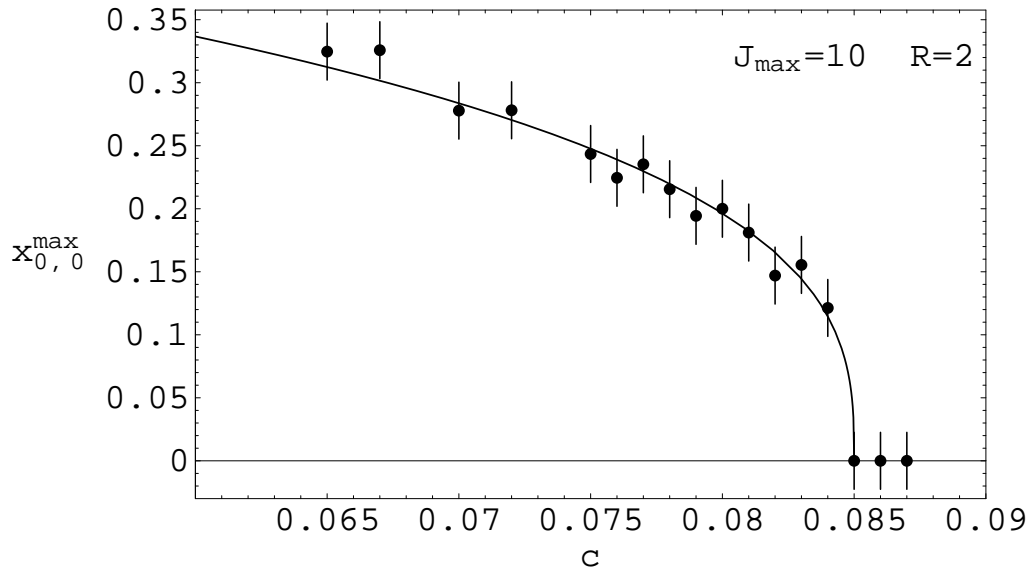


FIG. 6. $x_{0,0}^{\max}$ as a function of c for the theory defined by \mathcal{L}_- with $J_{\max} = 10$, $R = 2$.

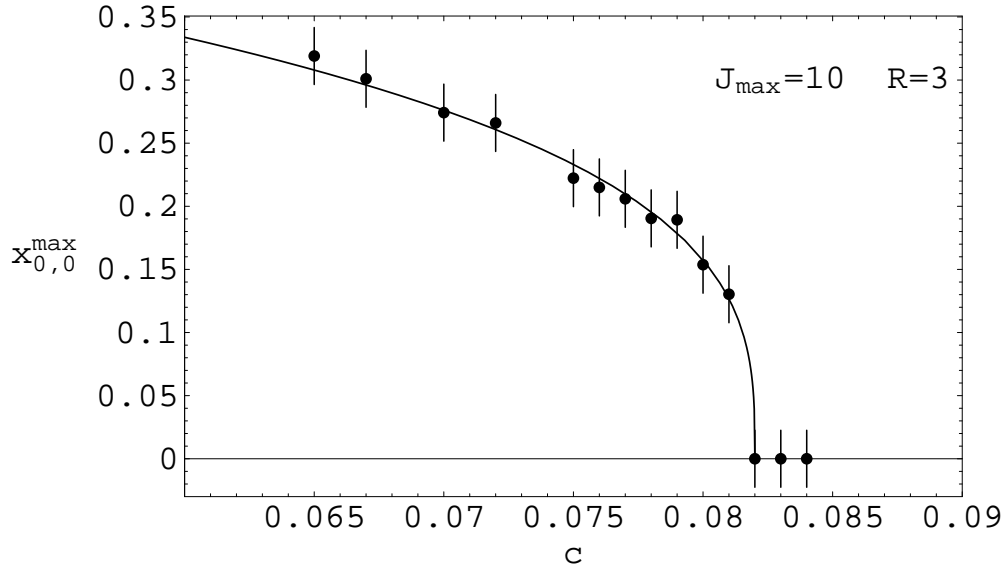


FIG. 7. $x_{0,0}^{\max}$ as a function of c for the theory defined by \mathcal{L}_- with $J_{\max} = 10$, $R = 3$.

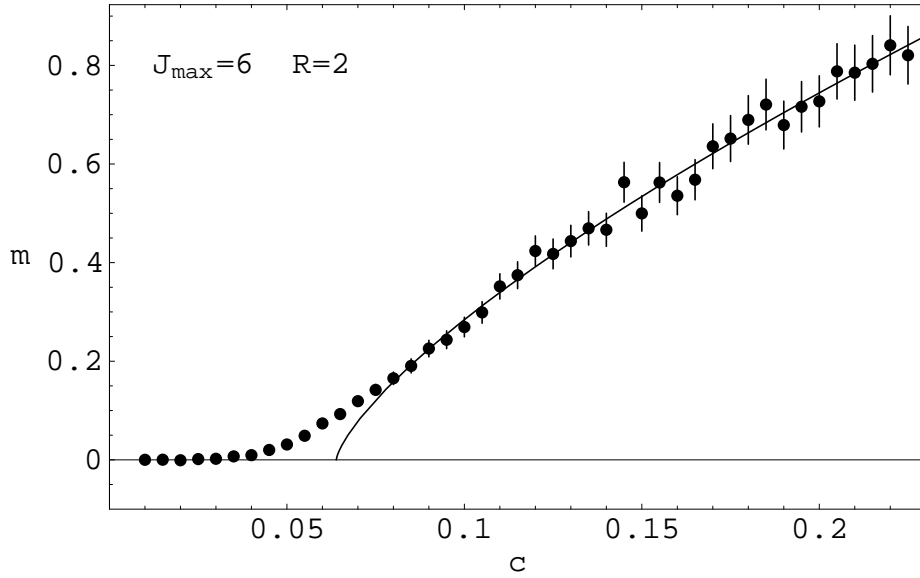


FIG. 8. m as a function of c for the theory defined by \mathcal{L}_- with $J_{\max} = 6$, $R = 2$.

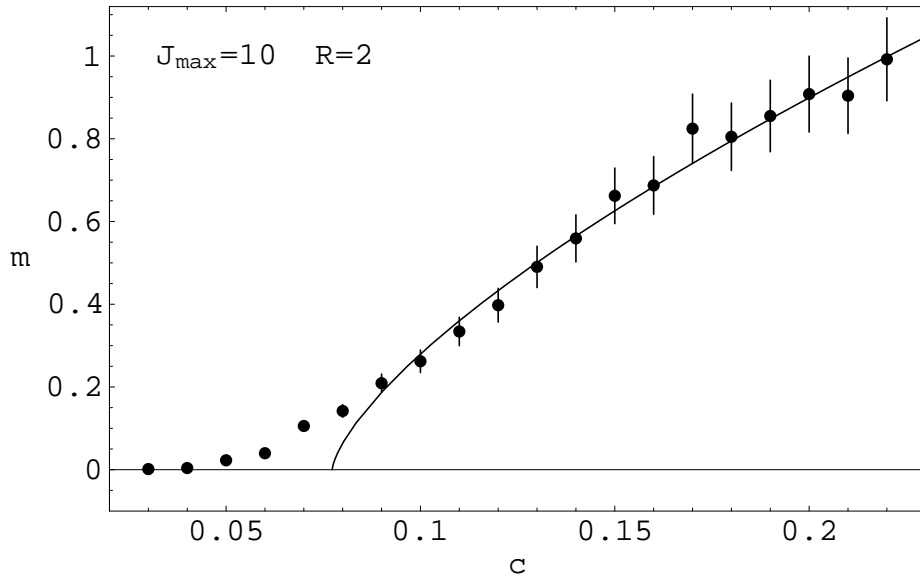


FIG. 9. m as a function of c for the theory defined by \mathcal{L}_- with $J_{\max} = 10$, $R = 2$.

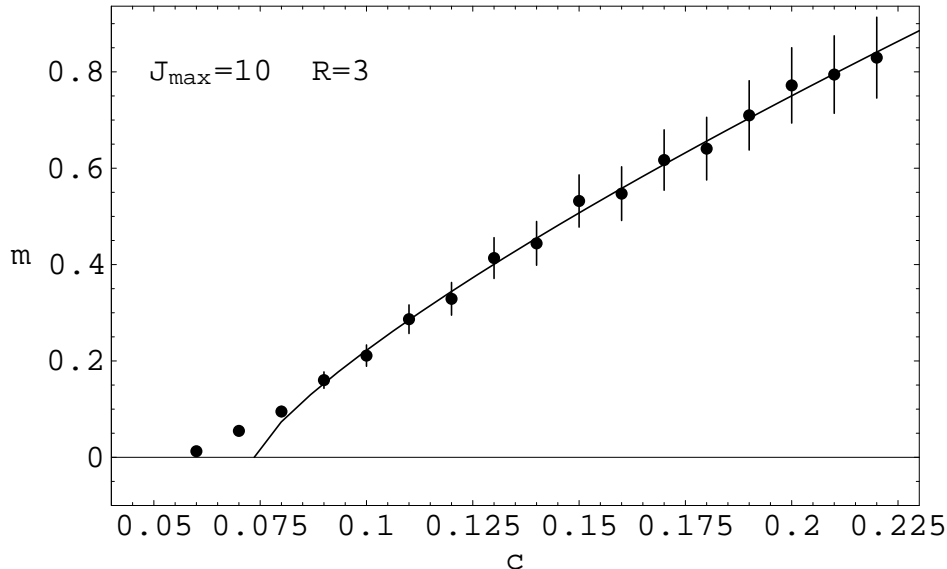


FIG. 10. m as a function of c for the theory defined by \mathcal{L}_- with $J_{\max} = 10$, $R = 3$.

$J_{\max} = 6$, $R = 2$; $J_{\max} = 10$, $R = 2$; and $J_{\max} = 10$, $R = 3$. The results are shown in Figs. 5-10. We find that at strong coupling the vacuum expectation value is zero but as we decrease the coupling strength the theory develops a nonzero vacuum expectation value and the physical mass vanishes. This clearly indicates that $\phi \rightarrow -\phi$ reflection symmetry, while manifest at strong coupling, is spontaneously broken at weak coupling.

The critical exponent β is defined by the behavior of the vacuum expectation value as we approach the phase transition from the broken-symmetry phase while the critical exponent ν is defined by the behavior of the physical mass m as we approach the phase transition from the symmetric phase. Therefore, we have fit the results using the parametrized forms

$$\langle 0^+ | \phi | 0^+ \rangle = a(c_{\text{crit}} - c)^\beta \quad \text{and} \quad m = b(c - c_{\text{crit}})^\nu. \quad (60)$$

The results of these fits are shown in Tables I and II.

The vacuum expectation value results are consistent with each other and with the recent calculations of β shown in Table III. Also note that $c_{\text{crit}} < 0.3522$. This is consistent with the finding of no phase transition for the \mathcal{L}_+ theory as discussed below Eq. (45).

The physical mass results are not as satisfying. We obtain values for ν which are consistently higher than expected for the three-dimensional Ising universality class as seen by a comparison with the recent calculations of ν shown in Table III. Furthermore, c_{crit} is found to be lower than the value obtained from the vacuum expectation value calculations. These difficulties arise because of a systematic error in the calculation of the physical mass very near the phase transition due to finite-size effects. This systematic error is apparent in each of Figs. 8-10 where the calculated values form a tail at small c . In the region of these tails the physical mass corresponds to a correlation length which is larger than the size of the system as given by R and so these points are of dubious validity. Therefore we must do our fits only for those points which are not too near the phase transition, *i.e.* for which $m \gtrsim \frac{1}{\pi R}$. This restriction makes it problematic to extract an accurate value for ν from fits to the

results. In the case of the vacuum expectation value calculations these finite-size effects are minimized as discussed below Eq. (57).

J_{\max}	R	a	c_{crit}	β
6	2	1.1(2)	0.081(4)	0.33(3)
10	2	1.2(1)	0.085(4)	0.34(3)
10	3	1.1(1)	0.082(4)	0.31(3)

TABLE I. Fit parameters for vacuum expectation value calculations.

J_{\max}	R	b	c_{crit}	ν
6	2	3.2(4)	0.064(6)	0.72(7)
10	2	3.8(7)	0.077(7)	0.69(9)
10	3	3.7(6)	0.074(7)	0.78(9)

TABLE II. Fit parameters for physical mass calculations.

Ref.	Method	β	ν
[6]	MC	0.3265(3)(1)	0.6294(5)(5)
[7]	HT	0.32648(18)	0.63002(23)
[8]	$d = 3$ exp.	0.3258(14)	0.6304(13)
[8]	ϵ -exp.	0.3265(15)	0.6305(25)

TABLE III. Recent results for the critical exponents of the three-dimensional Ising universality class.

VIII. SUMMARY

We have used the formalism of spherical field theory to analyze the phase structure of three-dimensional ϕ^4 theory. This analysis is intended as a demonstration that this new nonperturbative method can be successfully extended beyond two-dimensional theories. We find that for $\mu^2 > 0$ there is no spontaneous breaking of the $\phi \rightarrow -\phi$ reflection symmetry while for $\mu^2 < 0$ this symmetry is broken at weak coupling and is restored as the coupling strength is increased. We have calculated the critical coupling and the critical exponents β and ν which characterize the phase transition in the latter case by analyzing the behavior of the vacuum expectation value and the physical mass as functions of the coupling. Our result

for β , which was obtained from the vacuum expectation value analysis, is in agreement with recent calculations within the three-dimensional Ising universality class. However, our result for ν is somewhat larger than the results of these calculations. This is most likely due to finite-size errors which affect the physical mass analysis.

Several methods of improving this analysis come to mind. Our computations were performed with limited computing power: a 500 MHz Alpha workstation and a 350 MHz PC processor. Greater computing power could improve the analysis in two ways. First, the number of iterations performed within the Monte Carlo algorithm could be increased thereby reducing the statistical errors in the computations and increasing the precision of the results. Second, since the computation time scales roughly as J_{\max}^4 a substantial increase in computing power would allow us to take larger values for J_{\max} and R in order to reduce the systematic errors which arise due to these parameters being finite. Even with the limited computing power mentioned above, however, an improved analysis can be achieved with the method of periodic field theory [16] which uses a periodic-box mode expansion in place of the partial wave decomposition of spherical field theory and has the advantage of a time-independent hamiltonian. Improved calculations using this last approach are currently under way.

ACKNOWLEDGEMENTS

The author is grateful to Eugene Golowich and Dean Lee for many useful conversations and guidance. Support provided in part by the National Science Foundation.

REFERENCES

- [1] D. Lee, Phys. Lett. B439 (1998) 85.
- [2] S.F. Magruder, Phys. Rev. D14 (1976) 1602.
- [3] P. Cea and L. Tedesco, Phys. Lett. B335 (1994) 423; P. Cea and L. Tedesco, Phys. Rev. D55 (1997) 4967.
- [4] I. Stancu, Phys. Rev. D43 (1991) 1283.
- [5] A. Peter, J.M. Häuser, M.H. Thoma and W. Cassing, Z. Phys. C71 (1996) 515; A. Peter, W. Cassing, J.M. Häuser and M.H. Thoma, Z. Phys. A358 (1997) 91.
- [6] H.G. Ballesteros, L.A. Fernández, V. Martín-Mayor, A. Muñoz Sudupe, G. Parisi and J.J. Ruiz-Lorenzo, Phys. Lett. B441 (1998) 330.
- [7] M. Campostrini, A. Pelissetto, P. Rossi and E. Vicari, Phys. Rev. E60 (1999) 3526.
- [8] R. Guida and J. Zinn-Justin, J. Phys. A31 (1998) 8103.
- [9] C.J. Hamer, R.J. Bursill and M. Samaras, hep-lat/0002001.
- [10] M. Chaichian, A. Demichev, P. Prešnajder, hep-th/9904132.
- [11] D. Lee, Phys. Lett. B444 (1998) 474.
- [12] S. Fubini, A. Hanson and R. Jackiw, Phys. Rev. D7 (1973) 1732.
- [13] J. Avery, *Hyperspherical Harmonics: Applications in Quantum Theory* (Kluwer Academic Publishers, Dordrecht, The Netherlands, 1989).
- [14] Z. Wen and J. Avery, J. Math. Phys. 26 (1985) 396.
- [15] S.J. Chang, Phys. Rev. D13 (1976) 2778
- [16] P.J. Marrero, E.A. Roura and D. Lee, Phys. Lett. B471 (1999) 45.
- [17] I. Kosztin, B. Faber, and K. Schulten, Am. J. Phys. 64 (1996) 633.